JOURNAL OF PROPULSION AND POWER
Vol. 15, No. 6, November–December 1999

Magnetic Flowmeter Measurement of Pressure-Coupled Response of a Plateau Solid Propellant

E. H. Cardiff,* J. D. Pinkham,† and M. M. Micci‡
Pennsylvania State University, University Park, Pennsylvania 16802

A magnetic flowmeter was used to measure the pressure-coupled response of a plateau solid propellant. The magnetic flowmeter measures the one-dimensional acoustic gas velocity as a function of the height above the surface of a burning-propellant strand subjected to forced pressure oscillations. The unsteady gas velocity was measured by externally imposing a strong magnetic field in a region containing the propellant surface. The combustion product gas has sufficient ionization to be electrically conductive and generates an electrical potential proportional to the gas velocity in a direction perpendicular to both the magnetic field and the gas velocity and measured by two electrodes at the edges of the combustion gas flow. The position of the propellant surface relative to the measurement station was measured with an ultrasound transducer. The acoustic velocity, together with an acoustic pressure measurement as a function of distance above the burning propellant, was combined with a one-dimensional acoustic analysis of the flow to obtain the acoustic admittance at the propellant surface and thus the propellant response. Responses were measured at pressures up to 2000 psi (13.8 MPa) for frequencies between 300 and 1800 Hz. Results for a nonaluminized composite plateau propellant formulation are shown.

Introduction

THE ability to measure response functions for solid propellants is an important part of the examination of the stability of solid-propellant formulations. Pressure-coupled response functions are complex numbers that describe the interactions of various processes within the engine with respect to the unsteady pressure. Solid-propellant pressure-coupled response functions are measured by several experimental means, but most of these approaches have flaws. Among the methods used, the most common is the T-burner. However, the T-burner as well as the rotating valve burner, impedance tube, tangential mode burner, and modulated exhaust jet technique all use an indirect acoustic analysis to model the unsteady gasdynamics and combustion processes to obtain a response.[1,2] The reliability of these methods therefore hinges on the accuracy of the acoustic analysis used in the model.

In addition to the problems involved in the response-function determination, these methods also have physical limitations as to the frequencies and pressures at which measurements can be obtained. Only the variable area and pulsed T-burners can test at frequencies between 200 Hz and 10 kHz and at pressures up to 2000 psi (14 MPa). The impedance-tube method is capable of testing only up to 2400 Hz at a maximum pressure of 500 psi (3.5 MPa), and the rotating valve apparatus has only been operated to 800 Hz at 1500 psi (10.5 Mpa).

There are two techniques—microwave[1] and ultrasound[3]—that do not rely on an acoustic model to obtain the response function. However, the microwave technique only operates up to a frequency of 1 kHz at a maximum pressure of 1000 psi (7 Mpa) whereas the ultrasound method, which operates at a much lower frequency, is limited to 100 Hz.

The magnetic flowmeter possesses neither of these drawbacks. The magnetic flowmeter was proposed initially in 1951 as a means of measuring instantaneous liquid propellant flow rates as a rocket-motor combustion stability tool.[4] It is capable of directly determining the instantaneous velocity, which, when combined with an instantaneous pressure, allows a response function to be determined directly without reliance on an acoustic model. The method has been used to measure propellant pressure-coupled responses at pressures up to 2000 psi (13.8 MPa) and frequencies up to 20 kHz (Ref. 5), with the high-frequency signal analysis conducted by means of lock-in amplifiers.

Past experimental work has verified the magnetic flowmeter technique. Micci and Caveny[6] found the real part of the pressure-coupled response using a forced longitudinal wave (FLW) motor. A rotating gear was placed at the nozzle exit, enabling the FLW motor to induce acoustic oscillations within the chamber. Wilson and Micci[5] used a similar experimental setup to measure the real and imaginary parts of the pressure-coupled response as a function of height above the burning-propellant surface. The complex acoustic admittance of the burning-propellant surface was found from the nondimensional ratio of the velocity to the pressure oscillations from which the pressure-coupled response could be calculated. However, the calculated acoustic admittance was found from data that were taken over the short interval of time when the propellant passed the measurement station of the magnetic flowmeter. To obtain statistical confidence in the results, several tests at each frequency were needed. This can be avoided if simultaneous measurements of the location of the propellant burning surface are taken in conjunction with the pressure and velocity measurements.

This study combines the advantages of the magnetic flowmeter technique with simultaneous measurements of the height of the propellant burning surface by use of an ultrasound transducer. By knowing the distance between the electrodes, where the gaseous velocity was measured, and the burning surface along with concurrent pressure oscillation measurements, data can be taken as far as 0.93 in. (2.4 cm) above the burning surface. Thermal and viscous losses limit the distance above the propellant surface that useful measurements can be taken. The data are combined with an acoustic analysis of the standing wave above the surface of the propellant strand to obtain the pressure-coupled response. This allows response measurements to be made with greater accuracy.[7]

Magnetic Flowmeter Theory

The magnetic flowmeter functions according to Faraday's law. The ionized particles in the combustion gas flow past two electrodes that protrude into the flow. These electrodes are inserted in the propellant perpendicular to both a magnetic field and to the direction of the flow, as can be seen in Fig. 1. The voltage measured across

Received 23 April 1998; revision received 25 November 1998; accepted for publication 25 November 1998.

*Graduate Research Assistant, Department of Aerospace Engineering. Student Member AIAA.
†Graduate Research Assistant, Department of Aerospace Engineering.
‡Professor, Department of Aerospace Engineering. Associate Fellow AIAA.

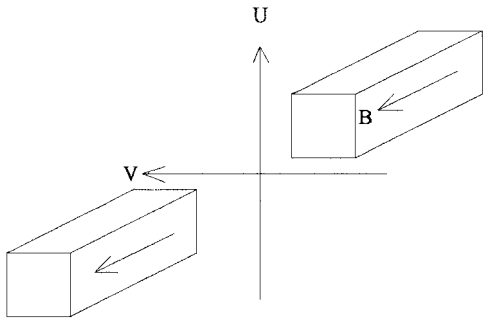

Fig. 1 Principle of Faraday's law used in the magnetic flowmeter.

the electrodes therefore allows the flow velocity to be determined according to Faraday's law:

$$U = V/\alpha BL \tag{1}$$

where U is the velocity of the flow, V is the voltage measured across the electrodes, B is the strength of the magnetic field, α is the end-shorting coefficient caused by the nonuniform magnetic field and having a value between 0 and 1, and L is the distance between the electrodes.

The electrodes were implanted in the propellant approximately 0.5 in. below the initial burning surface. As the burning surface burned down past the electrodes, the voltage across the two electrodes enabled the velocity to be obtained. The oscillatory pressure is created inside the magnetic flowmeter by means of a rotating gear placed above the aperture of the nozzle. A pressure transducer measures both the mean and the oscillatory pressures.

The measurement of both of these quantities directly allows the admittance of the burning surface to be calculated once the electrodes are exposed to the flow. The admittance is defined as the nondimensional ratio of the oscillatory velocity to the oscillatory pressure at the propellant surface:

$$A_b = \bar{\rho}\bar{a}[u'(0)/p'(0)] \tag{2}$$

where u' is the oscillatory velocity, $\bar{a}$ is the sonic velocity, p' is the oscillatory pressure, and $\bar{\rho}$ is the mean density.

The response function of the propellant is determined from the admittance by

$$R_p = (A_b/\gamma\bar{M}) + 1 \tag{3}$$

where $\bar{M}$ is the mean Mach number of the gases moving away from the burning surface, and R_p is the response function defined by

$$R_p = \frac{m_b'/\bar{m}_b + \Delta T'/\bar{T}}{p'/\bar{p}} \tag{4}$$

where m_b' is the oscillatory mass flow rate, $\bar{m}_b$ is the mean mass flow rate, $\Delta T'$ is the nonisentropic temperature oscillation, $\bar{T}$ is the mean temperature, and $\bar{p}$ is the mean pressure.

Experimental Approach

Chamber Setup

The experimental chamber used for testing was machined from a solid copper piece. The propellant cavity was 1.125 in. in diameter and 2 in. in height to accommodate the 1.4-in.-long propellant samples. The samples themselves were cast in phenolic-impregnated paper tubes to ensure end burning and to reduce coning. Before the burn, the samples were machined down to flatten the ends, thereby ensuring a good ignition surface on the top, and a good contact with the ultrasound coupling agent on the bottom. The chamber layout is shown in Fig. 2. Overpressurization is prevented by an emergency pressure-relief piston. When the maximum chamber pressure of 2500 psi was reached, a shear pin was designed to fail and release a piston and expose two exit ports with a total exit area of 0.0245 in.^{2} (0.158 cm^2).

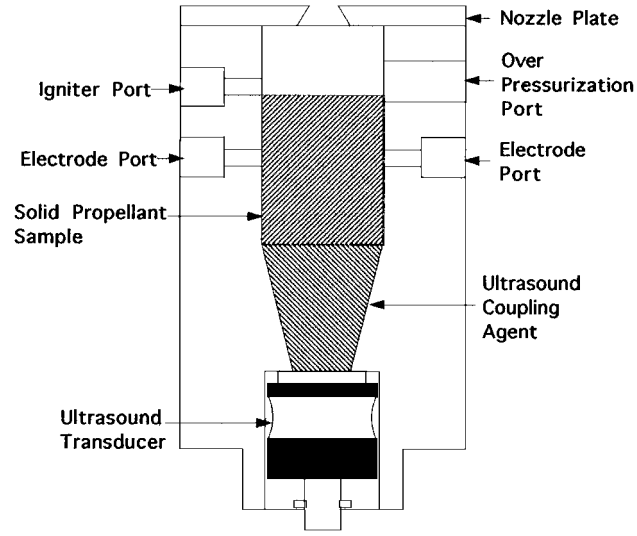

Fig. 2 Diagram of combustion chamber.

The chamber was sealed at the top with a copper nozzle piece that was machined to produce a convergent sonic exhaust at the desired chamber pressure and corresponding burn rate. To create an oscillatory pressure inside the chamber, a gear was placed directly over the sonic exhaust nozzle. The gears were selected and machined such that the face of the gear teeth matched the size of the choked nozzle orifice to ensure a near sinusoidal pressure oscillation at the desired frequency. This oscillatory pressure field was measured by a PCB Model 111A22 pressure transducer that measured both the oscillatory and mean pressure.

Two 2% thoriated tungsten electrodes placed perpendicular to the magnetic field and combustion gas flow measured the induced voltage in the ionized gas to allow a measurement of the gas velocity as described previously. These $\frac{1}{16}$-in.- (1.58-mm-) diam electrodes were placed 0.83 in. (2.1 cm) apart in a 1000-G magnetic field produced by a permanent horseshoe magnet.

A Panametric ultrasonic transducer and associated electronics provided the means to calculate the height of the electrodes above the burning-propellant surface. A coupling agent consisting of an epoxy resin and amine hardener was prepared before the test and poured into the conical section of the chamber, which, when cured, bonded with the bottom of the propellant. This allowed a clear transmission of the ultrasonic waves from the transducer placed flush against the coupling agent to the opposite (burning) side of the propellant.

Data Acquisition

Five channels of data were sampled for each 10-s test at 4096 Hz per channel with a Keithley Metrabyte DAS-20 A/D board. The five channels were the ultrasound propagation time, the mean pressure, the oscillatory pressure, the voltage across the magnetic flowmeter electrodes, and the gear-shaft frequency counter. The first signal, the ultrasound propagation time, was fed directly into the A/D board from the electronic device for ultrasound measurement obtained from ONERA.

The composite pressure signal from the pressure transducer was fed through a model 484B10 PCB voltage amplifier set at a gain of 10. The output of the amplifier was split to a sixth-order high-pass filter with a cutoff frequency of 200 Hz as all measurements were taken above 300 Hz. The high-pass filter removed the 60-Hz noise and the dc pressure trace, leaving the oscillatory pressure component, which was input along with the unfiltered mean pressure signal to the A/D board. To amplify the small voltages induced in the electrodes and to eliminate noise, a high-impedance differencing amplifier was used with a gain of 10. The shaft frequency was obtained by the light-emitting diode counter and multiplied by the number of teeth on the gear to give the gear frequency. Figure 3 shows a diagram of the data acquisition system.

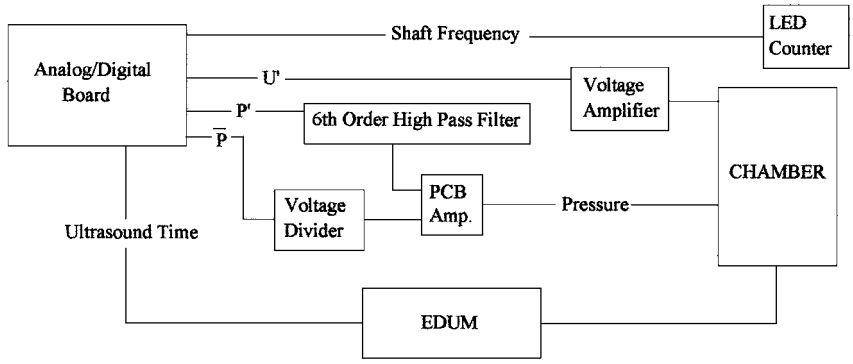

Fig. 3 Diagram of A/D system.

Data Analysis

The recorded raw data were input to a fast Fourier transform (FFT) program. The raw data were sampled at 4096 Hz per channel and formatted into blocks 0.25 s long of 1024 points for a total of 40 blocks and 10 s. The FFT used a discrete Fourier transform that produced a finite frequency resolution and maximum frequency.[8] The resolution and maximum frequency are determined by the sampling frequency and the total time of the test. The resolution for one data block is 4 Hz with a maximum detectable frequency of 2048 Hz. The FFT transformed the pressure and velocity time traces into the frequency domain while calculating the power-spectrum density (PSD) of the pressure and velocity signals and the cross spectrum-density (CSD) between the two signals.

A response-function program based on an acoustic model then was used to solve for the acoustic admittance as a function of height above the burning surface and, subsequently, the response function. The assumptions made in the development of the acoustic model were as follows[7]:

1) Both the mean flow and the acoustic oscillations are one-dimensional and normal to the propellant surface.

2) A constant cross-sectional area produced constant mean flow properties from the propellant surface to the entrance of the nozzle.

3) The mean flow properties, frequency of oscillation, burning-propellant surface area, magnetic flowmeter calibration constant, and propellant acoustic admittance remain constant during a test.

4) The mean and oscillatory flowfields are not affected by the magnetic field.

5) The magnitude of the mean flow properties are much greater than the magnitudes of the oscillatory flow properties and are isentropic.

The oscillatory components of pressure and velocity were derived from the small perturbation forms of the conservation of mass, momentum, and energy equations written as the sum of mean and sinusoidally fluctuating terms:

$$p'(x) = \left(Ye^{ikx/(1-\bar{M})} + Ze^{-ikx/(1+\bar{M})}\right)e^{i\omega t} \tag{5}$$

$$u'(x) = 1/\bar{\rho}\bar{a}\left(-Ye^{ikx/(1-\bar{M})} + Ze^{-ikx/(1+\bar{M})}\right)e^{i\omega t} \tag{6}$$

where $k = \omega/\bar{a}$, with ω being the oscillation frequency of the perturbation components. Defining an admittance A as a function of x following Eq. (2), the equations were combined to produce a nonlinear equation for the acoustic admittance at the propellant surface:

$$A_b = \frac{A(X)\cdot(X+1)+X-1}{A(X)\cdot(X-1)+X+1}$$

where

$$X = \exp[2ikx/(1-\bar{M}^2)] \tag{7}$$

The input data for the different positions produce a system of nonlinear equations for A_b, which are linearized by a Newton–Raphson technique. Then, the matrix of linear equations is solved iteratively by means of a least-squares method that allows a surface admittance and hence a response function to be calculated for the conditions input to the program.[7]

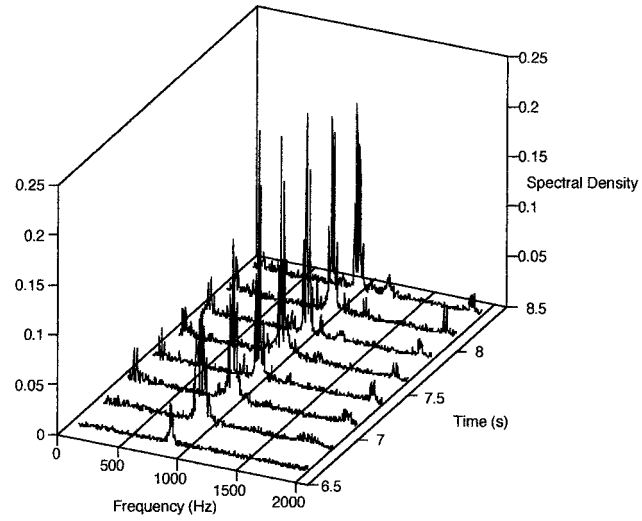

Fig. 4 Pressure PSD for a test at 300 psi and 900 Hz.

The FFT program provided values of the mean amplitude of the oscillatory pressure and velocity signals, and the phase difference between the two for each block of time for a range of frequencies calculated by the FFT. Values of the mean amplitude and phase of the oscillatory components corresponding to the forcing frequency along with the mean pressure and distance from the burning-propellant surface to the electrodes for each block of data were input to the response-function program. Three to twelve data blocks, depending on the burn time of the propellant strand, were used from each test to obtain a value of the response.

Results

The propellant tested was a composite nonaluminized plateau propellant supplied by Cordant Technologies. It was composed of 32.7% 200-μm and 53.3% 2-μm ammonium perchlorate particles by weight. The binder was hydroxyl-terminated polybutadiene. For pressures between 150 psi (1 MPa) and 500 psi (3.4 MPa) the pressure exponent n is approximately 0.28. Between 500 psi (3.4 MPa) and 1900 psi (13.1 MPa), n rises to 0.77, whereas for pressures between 1900 (13.1 MPa) and 2300 psi (15.8 MPa) a plateau is reached where $n = 0$.

For each propellant sample tested, the spectral analysis resulted in an averaged gain, coherence, and phase difference between the pressure and velocity signals, as well as 3 three-dimensional spectral plots of the pressure, velocity, and CSD magnitudes relative to time and frequency. The pressure signal from the spectral analysis is shown in Fig. 4. Here, data are shown between 6.5 and 8.5 s, during

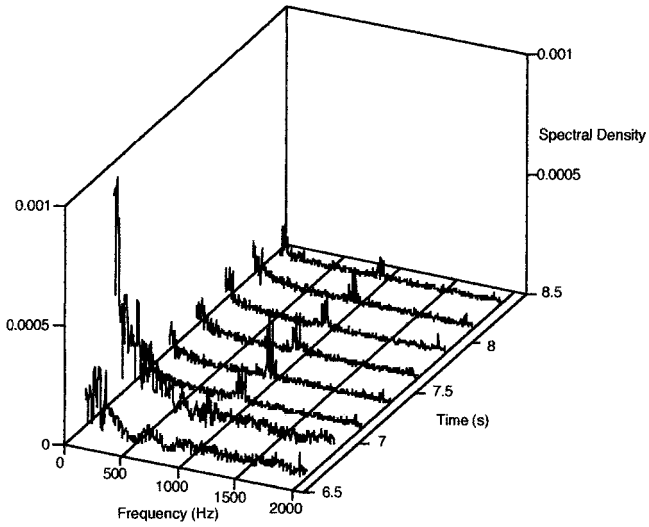

Fig. 5 Velocity PSD for a test at 300 psi and 900 Hz.

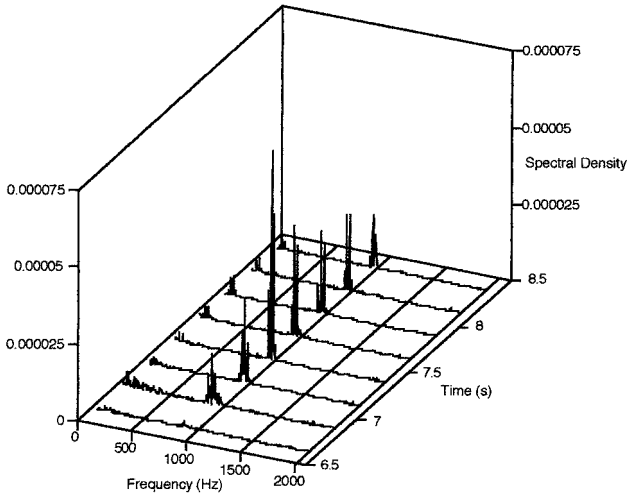

Fig. 6 CSD for a test at 300 psi and 900 Hz.

which the electrodes were exposed to the combustion flow. Each horizontal line represents a block of data averaged over 0.25 s of the test. The imposed forcing frequency of 900 Hz is clearly visible as the dominant signal, followed by the second harmonic at around 1800. Some low-frequency noise is also present.

Figure 5 shows the corresponding velocity PSD (VSD) as a function of frequency and time. The velocity PSD displays peaks at the same frequencies as the pressure spectra, showing both the induced frequency of 900 Hz and the second harmonic at 1800 Hz. Although the signal was significantly noisier, as expected, the frequencies were still clearly visible.

Figure 6 displays the CSD obtained from the correlation between the pressure and velocity signals. Pressure and velocity signals at similar frequencies are magnified whereas differing frequencies are minimized. Thus, the forcing frequency is evident from the CSD. The calculation of the CSD also provided the phase difference between the two signals, which was a crucial input to the response-function program. The CSD provided 9-, 7-, and 5-point averaged phase differences calculated from the real and imaginary parts of the complex CSD frequency signal for each block of data during the test. Equation (8) defines the phase error, which decreases for greater averaging:

$$\Delta\phi = \frac{\sqrt{1-\gamma_{pu}^2}}{|\gamma_{pu}|\sqrt{2n_p}} \tag{8}$$

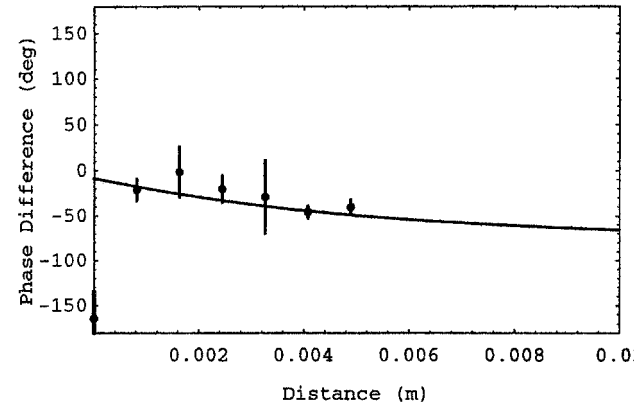

Fig. 7 Measured phase difference between the acoustic velocity and the pressure as a function of height above the burning-propellant surface (●) compared to acoustic model prediction (——).

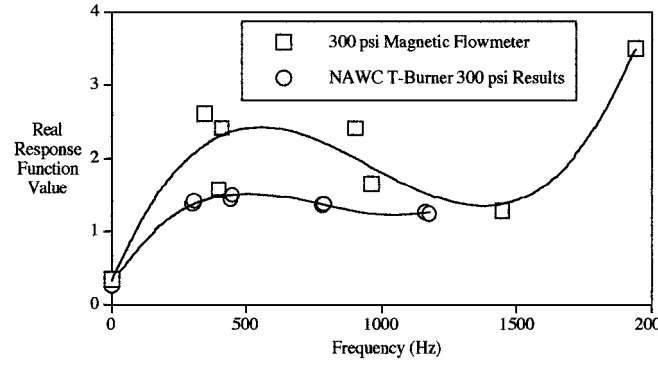

Fig. 8 Real part of the propellant pressure-coupled response as a function of frequency at 300 psi (2.1 MPa) obtained by the magnetic flowmeter and T-burner.[9]

The variable n_p defines the number of points over which the phase is averaged; in this case $n_p = 9$. The coherence function γ_{pu} predicts the error in the CSD phase calculation and is a number between 0 and 1. The coherence is a ratio of the averaged CSD to the product of the measured PSD and VSD. For a noiseless signal, the coherence equals 1.

Figure 7 shows the measured phase difference between the acoustic pressure and the velocity as a function of height above the burning-propellant surface. It is compared to the prediction by the acoustic model using the surface admittance deduced in part by the measured phase angles shown in the figure. The error bars on the measured phase are given by Eq. (8). It can be seen that the measured phase angles follow the acoustic model prediction within the obtained statistical error.

Figure 8 shows the magnitude of the real part of the pressure-coupled response vs frequency obtained by the magnetic flowmeter and the T-burner[9] at 300 psi (2.1 Mpa). The size of the symbols indicates the experimental error. The lines are third-order polynomial least-squares fits to the experimental data. Both the magnetic flowmeter and the T-burner measure the peak of the response to be at 500 Hz, with the magnetic flowmeter measuring a higher value. Above 1500 Hz the magnetic flowmeter is indicating a second response peak, characteristic of a bimodal composite propellant.[10]

Figure 9 shows the magnitude of the real part of the pressure-coupled response vs frequency obtained by the magnetic flowmeter and the T-burner at 1000 psi (7 Mpa). Both methods measured higher values for the real part of the response, but the T-burner measured the peak of the response at a lower frequency than at 300 psi whereas the magnetic flowmeter indicated it at a higher frequency. An increase in the frequency at which the maximum response occurs with increasing pressure normally is associated with the higher steady-state burning rate.

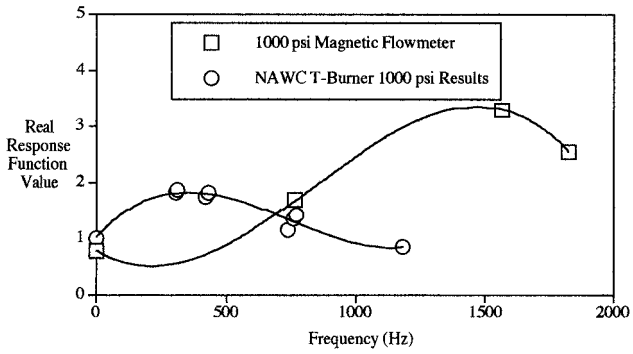

Fig. 9 Real part of the propellant pressure-coupled response as a function of frequency at 1000 psi (7 MPa) obtained by the magnetic flowmeter and T-burner.[9]

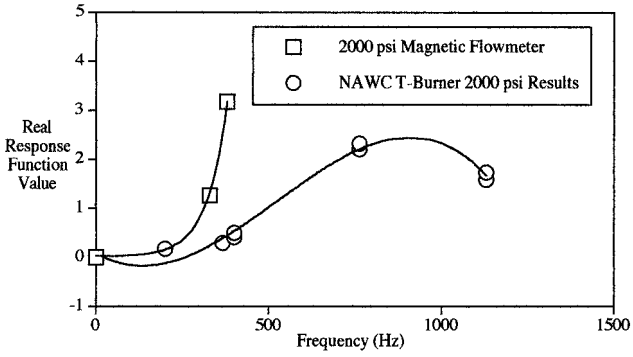

Fig. 10 Real part of the propellant pressure-coupled response as a function of frequency at 2000 psi (13.8 MPa) obtained by the magnetic flowmeter and T-burner.[9]

Figure 10 shows the magnitude of the real part of the pressure-coupled response vs frequency obtained by the magnetic flowmeter and the T-burner at 2000 psi (13.8 Mpa). Because of depletion of the propellant supply, not as many magnetic flowmeter data were taken at the highest pressure of 2000 psi. Once again, both methods measured yet higher values for the real part of the response. The T-burner now shows the peak of the response at a higher frequency (~900 Hz) than at 300 or 1000 psi, whereas the sparse magnetic flowmeter data show the response rising with frequency up to the maximum tested frequency of 380 Hz.

Conclusions

This study combined the acoustic velocity measurement of the magnetic flowmeter with an ultrasonic measurement of the location of the burning-propellant surface to provide a more accurate measurement of a solid-propellant pressure-coupled response. A one-dimensional acoustic analysis was used in conjunction with the magnetic flowmeter and ultrasound measurements to obtain a direct measurement of the burning-propellant acoustic admittance and thus the pressure-coupled response. Results were obtained for a nonaluminized composite plateau propellant that show characteristic behavior for the real part of the response function at three test pressures. These results demonstrate the capability of the magnetic flowmeter burner to obtain pressure-coupled response-function measurements at higher frequencies and pressures than are attainable by other methods.

References

[1]Strand, L. D., "Laboratory Test Methods for Combustion-Stability Properties of Solid Propellants," *Nonsteady Burning and Combustion Stability of Solid Propellants*, edited by L. DeLuca, E. W. Price, and M. Summerfield, Vol. 143, Progress in Astronautics and Aeronautics, AIAA, New York, 1992, pp. 689–718.

[2]Traineau, J.-C., Prevost, M., and Tarrin, P., "Experimental Low and Medium Frequency Determination of Solid Propellants Pressure-Coupled Response Function," AIAA Paper 94-3043, June 1994.

[3]Traineau, J.-C., and Kuentzmann, P., "Ultrasonic Measurements of Solid Propellant Burning Rates in Nozzleless Rocket Motors," *Journal of Propulsion and Power*, Vol. 2, No. 3, 1986, pp. 215–222.

[4]Jaffe, L., Coss, B. A., and Daykin, D. R., "An Electromagnetic Flowmeter for Rocket Research," NACA RM E50L12, 1951.

[5]Wilson, J. R., and Micci, M. M., "Direct Measurement of High Frequency Solid Propellant Pressure-Coupled Admittances," *Journal of Propulsion and Power*, Vol. 3, No. 4, 1987, pp. 296–302.

[6]Micci, M. M., and Caveny, L. H., "MHD Measurement of Acoustic Velocities in Rocket Motor Chambers," *AIAA Journal*, Vol. 20, No. 4, 1982, pp. 516–521.

[7]Cauty, F., Comas, P., Vuillot, F., and Micci, M. M., "Magnetic Flow Meter Measurement of Solid Propellant Pressure-Coupled Responses Using an Acoustic Analysis," *Journal of Propulsion and Power*, Vol. 12, No. 2, 1995, pp. 436–438.

[8]Bendat, J. S., and Piersol, A. G., *Engineering Applications of Correlation and Spectral Analysis*, 2nd ed., Wiley, New York, 1993, Chap. 3.

[9]Blomshield, F. S., and Stalnaker, R. A., "Combustion Response of Bi-Plateau Propellants," *34th JANNAF Combustion Subcommittee Meeting*, Publication 662, Vol. 4, Chemical Propulsion Information Agency, Columbia, MD, 1997, pp. 169–178.

[10]Murphy, J. J., and Krier, H., "Linear Pressure-Coupled Frequency Response of Heterogeneous Solid Propellants," *34th JANNAF Combustion Subcommittee Meeting*, Publication 662, Vol. 2, Chemical Propulsion Information Agency, Columbia, MD, 1997, pp. 69–78.